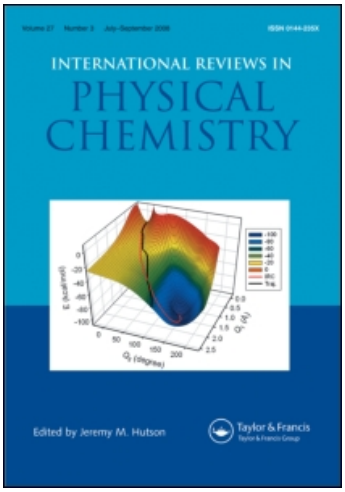

International Reviews in Physical Chemistry
Publication details, including instructions for authors and subscription information:
http://www.informaworld.com/smpp/title~content=t713724383

Organic semiconductors, conductors and superconductors

Hiroo Inokuchi[a]
[a] Institute for Molecular Science, Okazaki, Japan

To cite this Article Inokuchi, Hiroo(1989) 'Organic semiconductors, conductors and superconductors', International Reviews in Physical Chemistry, 8: 2, 95 — 124
To link to this Article: DOI: 10.1080/01442358909353225
URL: http://dx.doi.org/10.1080/01442358909353225

INTERNATIONAL REVIEWS IN PHYSICAL CHEMISTRY, 1989, VOL. 8, NOS. 2/3, 95–124

Organic semiconductors, conductors and superconductors

by HIROO INOKUCHI
Institute for Molecular Science, Okazaki, 444 Japan

The two major categories of organic solids are known to offer the present of good electrical conduction. The first group consists of charge-transfer complexes. Conductivity measurements on a large number of the charge-transfer complexes have been carried out. Among them, organic conductors (synthetic metals) and also organic superconductors have been discovered. The other group comprises single component materials; typical examples are polycyclic aromatic compounds and phthalocyanines. Their conductivities, generally speaking, are not as good as those of the charge transfer kind. We recently discovered a series of single component organic semiconductors having fairly good conductivity, which we called molecular fasteners. We also present, in this article, the experimental work on the ionization energy and carrier mobility measurements for the purpose of elucidating the conduction mechanism.

1. Introduction

Almost all saturated organic compounds are electrical insulators. Conjugated carbon–carbon double bonds, however, give rise to mobile electrons within the molecule, as typified by benzene. Aromatic compounds were found to exhibit unusual magnetic properties in the early 1900s, and graphite, a giant benzenoid network compound, was found to have the largest electrical conductivity, 10^5 S cm^{-1}, among non-metallic materials.

In the 1940s, phthalocyanines (Eley 1948), dyestuffs (Vartanyan 1948) such as cyanine dyes, and polycyclic aromatic compounds (Akamatu and Inokuchi 1950, Inokuchi 1951) were major objects of study, and the quantitative investigation of electrical conductivity of organic compounds was started. In the University of Tokyo, a systematic investigation of carbon blacks and graphites was carried out during the 1940s. At that time, it was already known that the basic structure of carbons contains condensed aromatic hydrocarbons. Realizing that these condensed polycyclic aromatic compounds could be considered to be ultra-micro-crystallites of carbons, Akamatu and Nagamatsu prepared carbon-like structures from polycyclic aromatic type vat-dyestuffs (violanthrone, isoviolanthrone and pyranthrone), by mixing their concentrated sulphuric acid solutions followed by aggregation in water (Akamatu and Nagamatsu 1947). To prepare the carbon-like aggregates, the mixing of different *molecular* sizes of polycyclic aromatics was essential. This work was the first introduction of polycyclic aromatic compounds into our studies.

As one of the systematic studies of carbons and graphite, their electrical conductivity and magnetic susceptibility were studied (Akamatu *et al.* 1956). Through the observation of the electrical conduction of carbon particles, we considered that the electron migration from one carbon particle to another should resemble that from one molecule to another in a molecular aromatic crystal.

Then, we started to measure the electrical conduction of polycyclic aromatic compounds (Akamatu and Inokuchi 1950). We selected violanthrone, isoviolanthrone and pyranthrone as typical examples of polycyclics (fig. 1).

0144–235X/89 $3·00

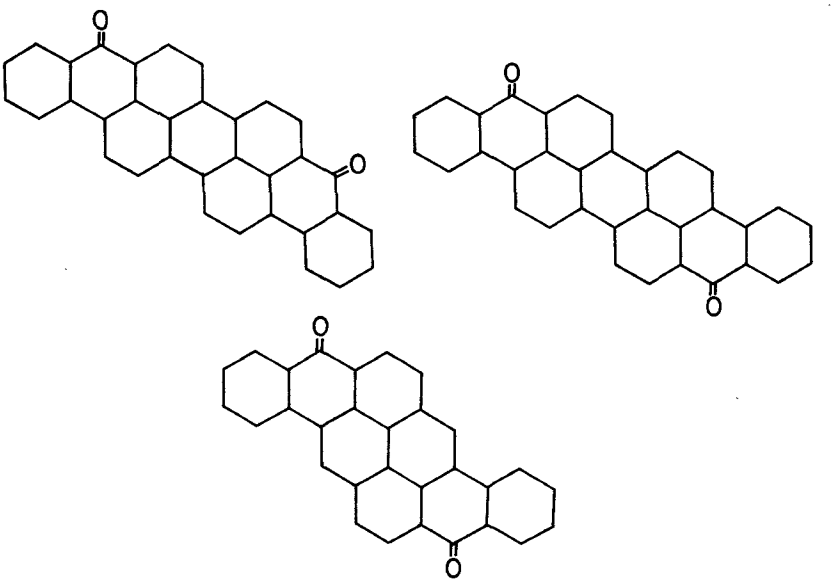

Figure 1. Violanthrone, isoviolanthrone and pyranthrone.

From the temperature dependency of conductivity measurements of the polycyclic aromatic series, it was found that conduction in these organic compounds appeared to be semiconductive. To confirm this electronic conduction of organic solids, we investigated intensively the photoconduction of the violanthrone series (Akamatu and Inokuchi 1952, Inokuchi 1954). From the accumulation of experimental results on the semiconductive character of this polycyclic aromatic series, in 1954 we presented a paper to the *Bulletin of the Chemical Society of Japan* entitled *Organic Semiconductors* (Inokuchi 1954). As described in section 5, we found a conductive organic complex, the 'perylene–bromine complex', in 1954 (Akamatu *et al.* 1954).

Two major categories of organic solids are known to offer the prospect of high electrical conduction. The first group consists of charge-transfer complexes such as the perylene–bromine complex. Consequently, conductivity measurements on a large number of the charge-transfer complexes (donor–acceptor complexes) have been carried out. The other group comprises single-component materials; typical examples are polycyclic aromatic compounds and also phthalocyanines. Generally speaking, their conductivities are not as good as those of the donor–acceptor kind.

A large number of studies on charge-transfer complexes have been carried out and their conductivity ranges from semiconductivity to superconductivity. As illustrated in figure 2, research progress in single-component organic semiconductors is rather slower than that concerning multicomponent organic systems, such as charge-transfer complexes.

However, from the theoretical research side, the study of conduction in single-component systems is desirable to enable us to analyse their conduction mechanism. We have recently discovered a series of single-component organic semiconductors having fairly good conduction, which we called 'molecular fasteners'. In the next few years, we would expect great progress to be made in the synthesis and study of single-component organic conductors.

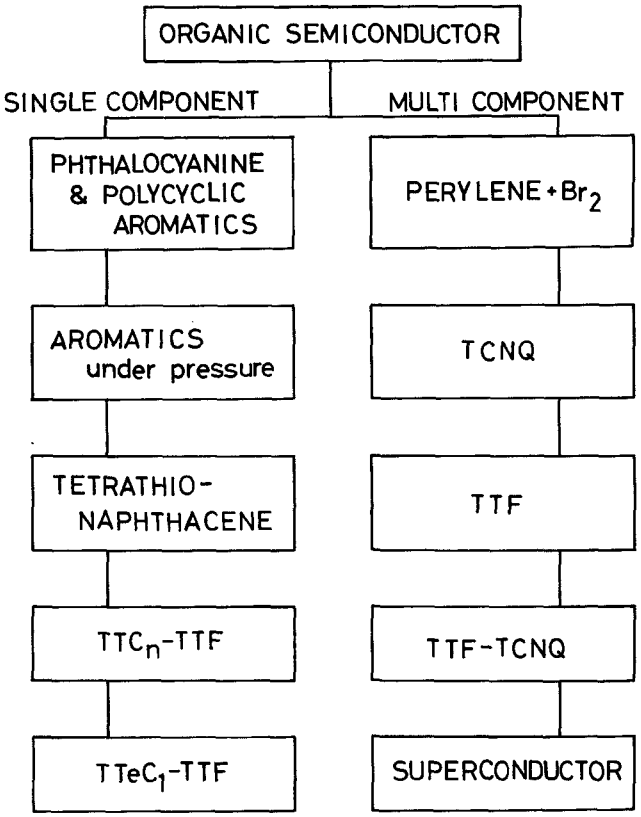

Figure 2. Research progress on organic semiconductors.

In this article, we will present a review of organic semiconductors, conductors and superconductors carried out in our school, together with some historical background.

2. Ionization energy of conductive organic solids

As a simple model, electronic conduction in molecular solids occurs by electrons jumping from one molecule to another. This concept is fundamental to the understanding of the conduction mechanism. Among the physical properties of organic materials, isolated molecules and solids, ionization energy is a predominant parameter in discussing electrical and electronic phenomena in organic solids, such as charge-carrier generation, injection, charge-transfer phenomena and also the polarization effect.

Concerning the observation of ionization energy, our first work was concerned with the photoemission from violanthrene–Cs charge transfer complexes (Inokuchi and Harada 1963). The photocells used in this experiment, as illustrated in figure 3, were constructed from films of violanthrene–Cs charge transfer complexes. Figure 4 illustrates the spectral response of photoemissive current: the current was a curve falling gradually from the short-wave length side to the long-wave length side, and no maximum of response was found in the wavelength region of 300–700 μm.

Following this preliminary work, we started to observe the ionization energy of molecular solids and also charge-transfer complexes using their photoemission phenomena. Firstly, the photoemission (external photoelectric effect) of thin films of polycyclic aromatic compounds was studied in the vacuum ultraviolet region. The ionization energy of organic solid (I_s) was estimated from spectral distribution of the quantum yield (Y). The numerical value of I_s was determined by extrapolation to a quantum yield of 10^{-8} electrons per incident quantum (Harada and Inokuchi 1966). Later (Kochi *et al.* 1970), we introduced the following equation to obtain the ionization energy;

$$Y \propto (h\nu - I_s)^{1/3},$$

where $h\nu$ is incident light energy. Further, we applied photoelectron spectroscopy to the study of a polycyclic aromatic, naphthacene, in the vacuum ultraviolet region, using an a.c. modulated retarding potential method (Hirooka 1973). The energy distribution curves (EDCs) of naphthacene are illustrated in figure 5. The introduction of this photoelectron spectroscopic method proved very advantageous for the estimation of ionization energy and important related factors.

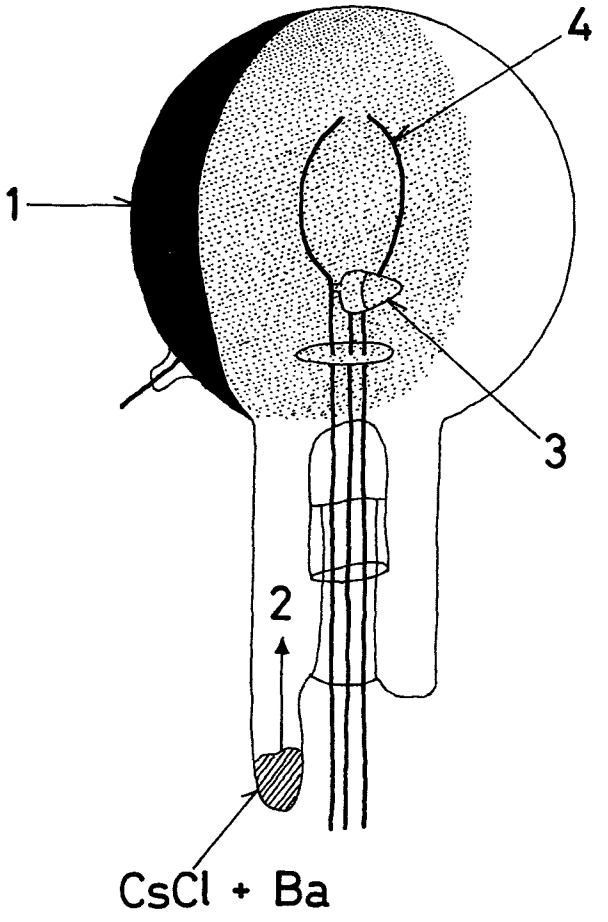

Figure 3. A photocell to make a complex between alkali-metal and aromatics and observe a photoemission: (1) complex film, (2) vapour of Cs metal, (3) electric heater and (4) collector.

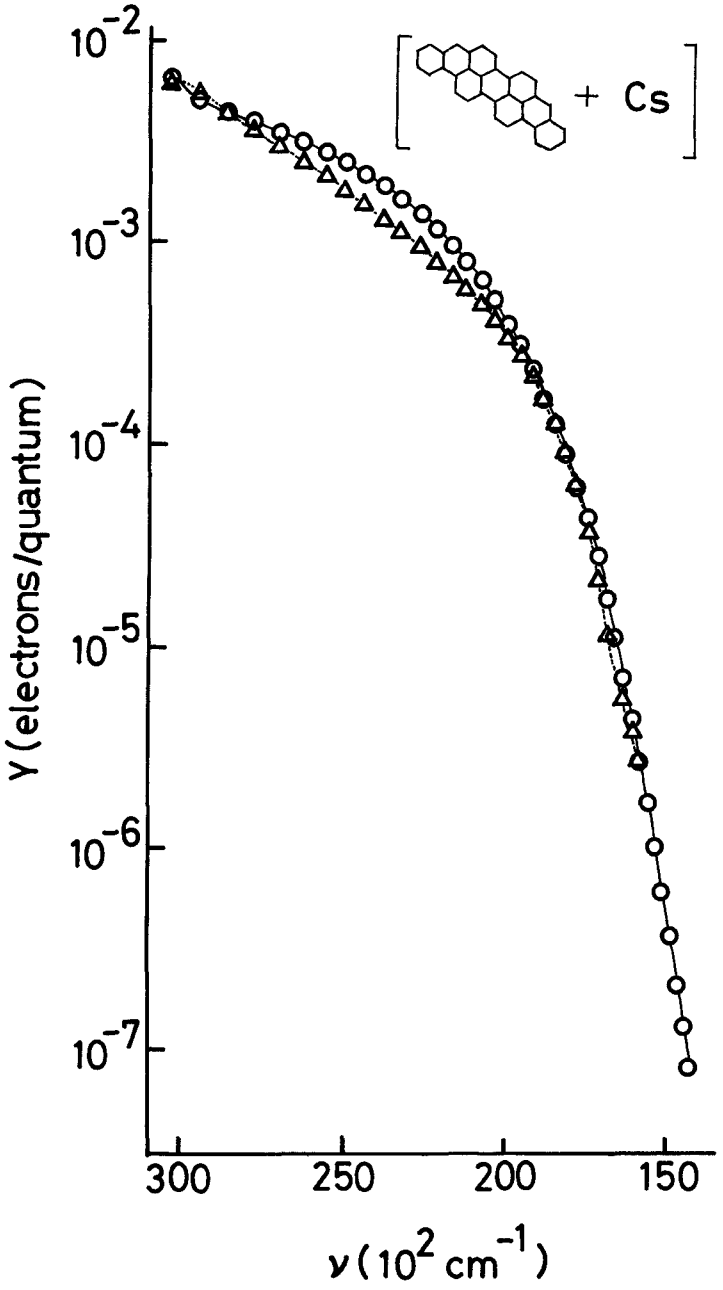

Figure 4. Spectral response of the photoelectric quantum yield (Y) in electrons/quantum^{-1} for violanthrene–Cs complex. △ observed at liquid nitrogen temperature, ○ at room temperature.

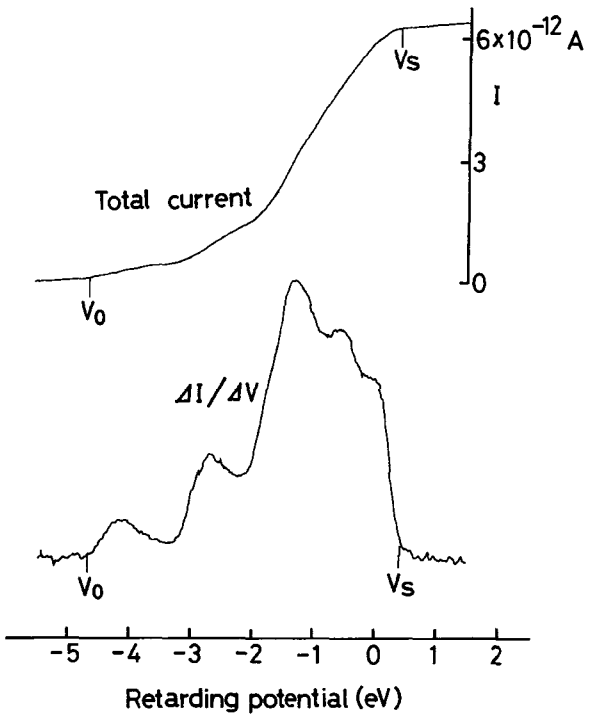

Figure 5. Energy distribution curve (EDC) for naphthacene: The current–voltage characteristic curve (above) and its derivatives (below) for an incident photon energy $h\nu = 10{\cdot}33$ eV.

2.1. *Photoelectron spectroscopy (UPS) of organic solids*

As illustrated in figure 6, the spectral response of naphthacene shows a distinctive pattern. The important features of UPS experiments are as follows:

(1) An accurate determination of the absolute binding energy relative to the vacuum level is required (Inokuchi *et al.* 1987).
(2) Surfaces are less active than those of inorganic solids.
(3) Vapour pressures are higher than those of inorganic solids.
(4) Radiation damage must be considered.
(5) Surface charging due to the insulating character must be considered.

An accurate determination of binding energy relative to the vacuum level is important, since comparison with gas-phase UPS gives a measure of the solid-state relaxation effect. As shown in figure 6 (Seki *et al.* 1973), which is a more accurate curve as compared with figure 5, the molecular identity in the solid state is reflected by the electronic structure of molecular solids bound by van der Waals forces between rigid molecules; this yields a good one-to-one correspondence of UPS spectra between the gas phase and the solid phase. This good relationship indicates that photoemission from molecular solids can be regarded as the photo-ionization of the molecule embedded in the solid. This idea is the basis for interpreting the solid-state UPS spectra.

Solid state effects appear in the UPS spectra as (i) the lowering of the ionization energy and (ii) peak broadening. The former arises from the stabilization of the

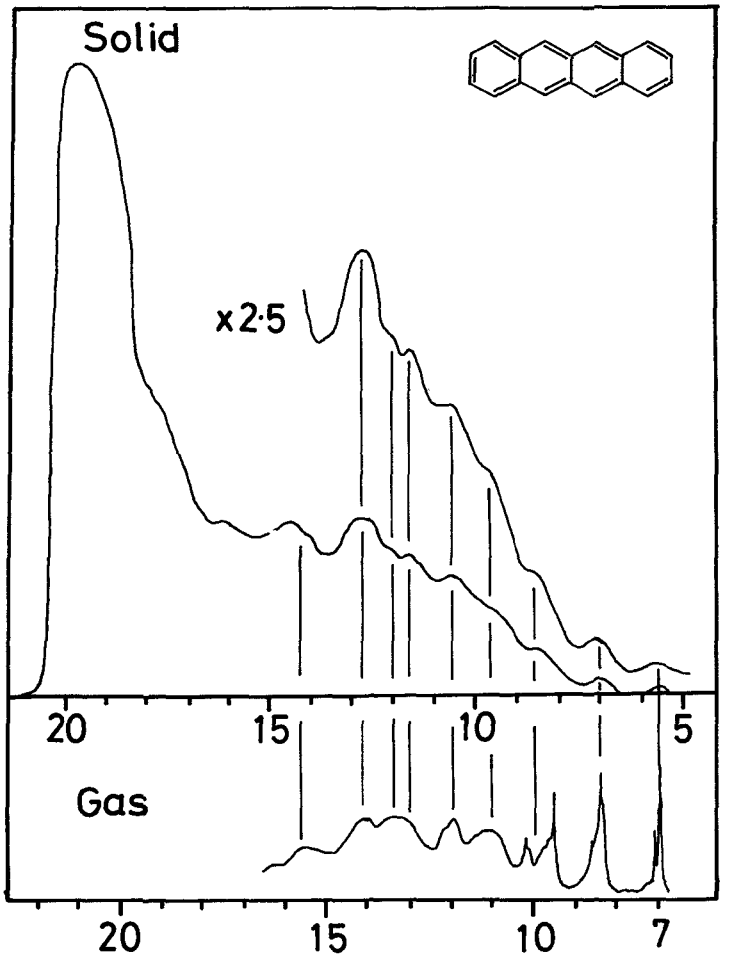

Figure 6. Comparison of photolectron spectroscopical patterns of naphthacene in gaseous and solid states for $h\nu = 21{\cdot}2$ eV.

photoinduced cation by the electrostatic polarization of the surrounding molecules; the difference between ionization energies of solid state and molecular state is for practical purposes called polarization energy. Table 1 summarizes the ionization energy (I_s) and the polarization energy (P_+) of typical examples from among 90 organic compounds observed, with gas-phase ionization energy (I_g) (Inokuchi *et al.* 1987b). The polarization energy is interpreted in terms of two factors; one is molecular packing in the solid and the other molecular polarizability (Sato *et al.* 1981). As a result, P_+ values become large when molecules are closely packed and/or the polarizability of the surrounding molecules is large. As seen in table 1, the aromatic hydrocarbons have almost constant P_+-values of 1·7 eV, since the increase of molecular size, which causes a decrease in the molecular packing density, balances with a parallel increase of the polarizability. Compounds including highly polarizable atoms (halogens) have large P_+, while molecules with intricate geometrical structures (e.g. rubrene) show small P_+ values due to the loose molecular packing. Such a wide spread of P_+ values

demonstrates the difficulty in predicting the electronic structure in the solid state. However, the two physical constants, I_s and P_+, are quite good guide-lines for making single component organic semiconductors and also for the preparation of charge-transfer materials.

2.2. *Ionization energy for multicomponent systems*

A typical example of multicomponent systems is a charge-transfer complex: the complex can be regarded as a binary system where component molecules are mixed at the molecular level. It is well recognized that the degree of charge transfer in molecular complexes depends upon the combination of the ionization energy of the donor and the electron affinity of the acceptor. The actual application of ionization energy will be described in section 5.

Table 1. Photo-ionization energy of molecule (I_g) and solid (I_s) of organic materials determined by photoelectron spectroscopy and their polarization energy (Inokuchi *et al.* 1987b).

Compound	I_g (eV)	I_s (eV)	P_+ (eV)
Hexane	$10{\cdot}2_5$	$8{\cdot}5_5$	1·7
Neopentane	10·2	8·7	1·5
Tetramethylsilane	9·79	8·2	1·6
Stearic acid (crystalline)	[10·0]	8·0	2·0
Naphthalene	8·12	6·4	1·7
Anthracene	7·42	5·75	1·67
Naphthacene	6·89	5·10	1·8
Pentacene (crystalline)	6·58	4·85	1·7
(amorphous)		5·15	1·43
Chrysene	7·51	5·8	1·7
Pyrene	7·37	5·8	1·6
Perylene	6·90	5·2	1·7
Coronene	7·25	5·52	1·7
Violanthrene A	6·42	4·9	1·6
p-Terphenyl	7·9	6·1	1·8
Tetrabenzo[*a,cd,j,lm*]perylene	6·58	$5{\cdot}3_4$	$1{\cdot}2_4$
Tetrabenzo[*de,hi,op,st*]pentacene	6·13	$4{\cdot}9_8$	$1{\cdot}1_5$
Rubrene	6·41	5·3	1·1
Cu-phthalocyanine (α-form)	6·15	$4{\cdot}8_8$	$1{\cdot}2_7$
(β-form)		$4{\cdot}6_2$	$1{\cdot}5_3$
3-ethyl-5-[3-ethyl-2-benzothazolinylidene] rhodanine (merocyanine dye)	[6·98]	$5{\cdot}5_5$	$1{\cdot}4_3$
Tetrathionaphthacene	6·07	4·4	1·7
Tetrathiafulvalene (TTF)	6·4	5·0	1·4
Tetramethyl TTF (TMTTF)	6·27	$4{\cdot}8_4$	$1{\cdot}4_3$
Bibenzo TTF (DBTTF)	6·68	4·4	2·3
Bis(ethylendithiolo) TTF (BEDT-TTF)	6·21	$4{\cdot}7_8$	$1{\cdot}4_3$
Tetraselenafulvalene (TSF)	6·68	$4{\cdot}9_9$	$1{\cdot}6_9$
Tetracyanoquinodimethane (TCNQ)	9·5	7·4	2·1
Hexachlorobenzene	8·98	7·3	1·6
Hexaiodobenzene	7·90	5·9	2·0
p-Chloranil	9·74	8·1	1·6
p-Iodanil	9·58	5·6	3·0
Iodine	9·26	$6{\cdot}3_4$	$2{\cdot}9_2$
Tetraiodemethane	9·00	$5{\cdot}5_0$	$3{\cdot}5_0$
Tetraiodoethylene	8·57	$5{\cdot}0_4$	$3{\cdot}5_3$

3. Mobility measurements of conductive organic solids

In an organic molecular crystal system, a relatively small intermolecular resonance interaction leads the difficulty in the coherent itinerant motion of charge carriers throughout the solid, and the electron–phonon interaction becomes crucially important for the electronic state of the organic solids.

In this consideration, the small polaron theory developed by Holstein (1959a) should be a starting point for the theoretical approach to mobility in molecular materials. The motion of a small polaron is strongly dependent on the temperature at which it is observed. At sufficiently low temperatures it can be described in terms of motion in a small polaron band, the width of which is a decreasing function of increasing temperature since it associates with not only electronic but also vibrational overlaps (Holstein 1959b). Consequently, the drift mobility of carrier will increase with decreasing temperature, like in the band picture.

The electric current I flowing through solid state materials is formulated as

$$I = ne\mu_D F,$$

where n, e, μ_D and F are the charge-carrier density, elementary charge, drift mobility and applied electric field respectively. The first report of μ_D measurements in organic molecular crystals was published for anthracene single crystals by LeBlanc (1960), and at almost the same time by Kepler (1960), also for anthracene. This method is the so-called 'time-of-flight' measurement, and is still a standard method for the measurement of μ_D in organic crystals. Recently, the light source has been replaced by many kinds of short-pulse lasers, and a transparent electrode of tin-oxide glass or quartz (Nesa) is now usually used. Table 2 lists the numerical value of mobility of organic solids, including those observed by us (Maruyama 1989). A more complete list up to 1982 was reported by Schein and Brown (1982).

As mentioned in table 2, the well established results for organic molecular crystals are, as for the magnitude of the mobility μ_D, independent of the particular materials,

$$\mu_D \sim 1\ \mathrm{cm^2\ v^{-1}\ s^{-1}}$$

within an order of magnitude at room temperature, and μ_D is almost always temperature dependent

$$\mu_D \propto T^{-n}, \quad n = 0\text{–}3.$$

As an exceptional example, we will present μ_D of molecular fastener (see TTC_9–TTF in table 2) in the next section. Further, we also found a high-mobility organic semiconductor, $TTeC_1$-TTF in table 2, having quasi-covalent bonds (Inokuchi *et al.* 1987a).

In this review, we present two of our mobility studies. One is a more careful observation of charge-carrier mobility and the other is the measurement of mobility under high pressure.

In the measurement of drift mobilities by the 'time-of-flight' method, we must consider the space-charge polarization effect. We employed a pulsed electric field and measured the change in photoresponses according to the light-delay times (Maruyama and Inokuchi 1967). No distinct reduction of photoresponse, however, was found, and the mobility value was nearly the same as that obtained by measurement with the conventional d.c. field as mentioned above. To measure the microscopic mobility in anthracene crystal, we also measured the photo-Hall effect of anthracene by means of the Redfield–Kobayashi–Brown method (Redfield 1954, Kobayashi and Brown 1959,

Table 2. Charge-carrier mobilities in organic molecular solids (Maruyama 1989).

	Sign of carrier	Orientation	Room temperature mobility ($cm^2 V^{-1} s^{-1}$)	$\mu \propto T^{-n}$ n	Temperature range (K)
Anthracene	+	*a*	1·13	−1·5 (2)	78–300
	+	*b*	2·07	−1·5 (2)	78–300
	+	*c′*	0·73	−1·5 (2)	78–300
	−	*a*	1·73	−1·57	78–300
	−	*b*	1·05	−0·84	78–300
	−	*c′*	0·39	−0·16 (2)	78–300
Benzene	−	*a*	1·5 (278 K)	−2·0	173–278
Biphenyl	−	*a*	0·42	−1·0	135–300
	−	*b*	1·25	−1·25	76–300
	−	*c′*	0·51	−1·0	100–250
p-diiodbenzene	+	*a*	12·0	−0·5	250–300
	+	*b*	4·0	0	250–350
	+	*c*	1·7	−0·8	250–320
Durene	+	*ab*	5·0 (120 K)	−2·5	130–300
	+	*c′*	0·1	−2·8	130–300
	−	*ab*	8·0 (120 K)	−2·5	130–300
Iodoform	+	Parallel to sixfold axis	0·18	$0·2 < n < 1$	270–340
	+	Sixfold axis	0·7		270–340
Naphthacene	+	*c′*	0·85	$-3 < n < -2$	300–350
Naphthalene	+	*a*	0·90 (10 K)	−2·9 (1)	78–300
	+	*b*	1·5	−2·5 (3)	78–300
	+	*c′*	0·30	−2·82 (2)	78–300
	−	*a*	0·65	−1·52 (5)	78–300
	−	*b*	0·63	$\exp(9 \pm 1\ meV/kT)$	75–100
	−	*c′*	0·44	$\exp(6·6 \pm 0·1\ meV/kT)$	31–100
				0·1 (1)	100–325
Perylene	−		2(30 K)	−1·7	30–300
Phthalocyanine	+		1·1 (373 K)	$-1·6 < n < -1·1$	300–630
(β-form)	−		1·2 (373 K)	$-1·6 < n < -1·3$	300–630

Pyrene	+	*ab*	0·7	−1·6	260–350
	+	*c′*	0·5	−1·3	260–350
	−	*ab*	0·7	−1·5	260–350
	−	*c′*	0·5	−2·0	260–350
p-terphenyl	−	*a*	0·34	−2·5	70–180
				−0·5	180–300
	−	*b*	1·2	−2·5	90–180
				−0·7	180–300
	−	*c′*	0·25		160–300
	+	*c′*	0·8		160–300
o-terphenyl	−	*b*	3	exp(−140 meV/kT)	210–270
TCNQ	−	(001)	0·65	−1·0	210–350
$TSeC_2$–TTF	+		1·4		
	−		1·7		
TTC_9–TTF	+		8·7		
	−		19		
$TTeC_1$–TTF	+		28·5		
	−		18·6		
TTF–TCNQ			3 (54 K)		
HMTSF–TCNQ	−		4×10^4 (4 K)		
	+		$1{\cdot}2 \times 10^4$ (4 K)	Hall effect	
$(TMTSF)_2PF_6$			10^5–10^6 (4 K)		
Anthracene	+		−35–200		
	−		−2–50		
Polyvinyl carbazole	+		10^{-6}		
PVK : TNF	+		10^{-8}–10^{-5}		
	−		10^{-8}–10^{-6}	Polymers (insulating)	
Polyethylene	+		10^{-10}		

Maruyama and Inokuchi 1967). The observed Hall mobility was in the range of 25–200 $cm^2 V^{-1} s^{-1}$. This fairly large Hall mobility will be explained in terms of the multiple-trapping effect in organic crystals.

In 1967, we also measured the drift mobility under high pressure up to 7·4 kbar for an anthracene single crystal (Kajiwara *et al.* 1967). Figure 7 shows the pressure dependence of the μ_D for an anthracene single crystal. All the values were for electron mobility, because the hole mobility was difficult to measure. The μ_D curves were quite specific. The electron μ_D along the c' axis was approximately constant up to a pressure of 6·6 kbar.

The electron mobility along the a axis increased linearly with pressure up to 3·0 kbar, and varied superlinearly with pressure in the region between 3·0 and 5·0 kbar. Above 5 kbar, the rate of increase declined. In the case of the b axis, the general behaviour of the mobility as a function of the applied pressure was similar to that measured along the a axis. We have also measured the elastic constants of an anthracene single crystal (Danno and Inokuchi 1968). In this work, the thirteen elastic constants, C_{ij}, and the elastic compliances, s_{ij}, of monoclinic single-crystal anthracene, were determined from sound velocities by the ultrasonic pulse method at room temperature.

In this experiment, a zone-refined anthracene single crystal, 20 mm × 20 mm × 10 mm, was cut along the cleavage plane with a blade: the cleavage plane lies parallel to the ab crystal axes. The direction of the b axis on the cleavage plane was determined by the double-refraction method.

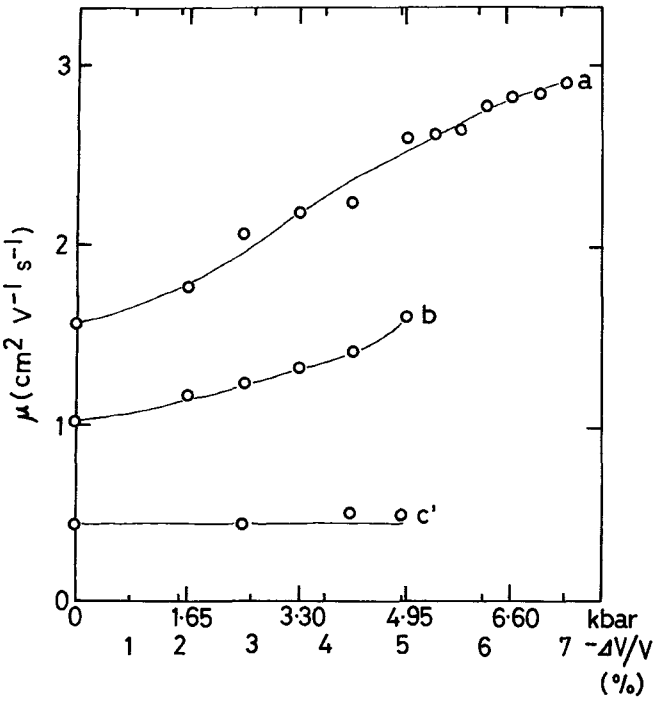

Figure 7. Electron mobility of anthracene under high pressure. Curve a is the relation along the a axis, curve b along the b axis, curve c' along the c' axis.

The elastic constants and elastic compliances of anthracene are listed in table 3. From these observed values, the linear compressibility (β) along [100], [010] and [001] are:

$$\beta_{[100]} = 12{\cdot}7 \times 10^{-12}\,\mathrm{cm^2\,dyn^{-1}},$$
$$\beta_{[010]} = -4{\cdot}41 \times 10^{-12}\,\mathrm{cm^2\,dyn^{-1}},$$
$$\beta_{[001]} = 3{\cdot}59 \times 10^{-12}\,\mathrm{cm^2\,dyn^{-1}}.$$

The elastic constants of anthracene are one-tenth and/or one-hundredth those of covalent crystals, ionic crystals and metals. These observed constants are very important factors for the understanding of the physico-chemical properties of organic solids, for instance the effect of pressure on electrical conduction. The pressure dependence of μ_D is also one typical example. The behaviour of the pressure dependency corresponded closely with this compressibility ratio. The absence of pressure dependence of μ_D along the c' axis was supported by this compressibility data. In the latter half of the 1970s, new developments in measuring techniques permitted the measurement of the temperature dependence of μ_D down to below 77 K. This wide range of data has led to much theoretical discussion on charge transport mechanism in organic semiconductors.

4. Ionization energy and charge mobilities of the molecular fastener

As mentioned in the introduction, we are currently studying novel *single-component* organic semiconductors. In this section, we present a new strategy for the fabrication of molecular assemblies in such a fashion that organic π molecules can pile up one upon another so tightly that the system shows a high conductivity, even as a single component (Inokuchi *et al.* 1986).

Figure 8 shows the molecular structure of these novel organic semiconductors, alkylthio-substituted tetrathiafulvalene (hereafter referred to as TTC_nTTF). The electrical conductivity of single crystals of this series ($n = 1$–18) have been measured in a vacuum of 10^{-4} Pa with the two probe method using gold paste electrodes. Table 4

Table 3. Elastic constants ($10^{10}\,\mathrm{dyn\,cm^{-2}}$) and elastic compliances ($10^{-12}\,\mathrm{cm^2\,dyn^{-1}}$) of anthracene.

Elastic constants						
C_{11}	C_{12}	C_{13}	C_{15}	C_{22}	C_{23}	C_{25}
8·92	4·63	4·49	−2·58	13·8	8·44	−2·59
C_{33}	C_{35}	C_{44}	C_{46}	C_{55}	C_{66}	
17·0	−2·88	2·42	1·14	2·84	3·16	
Elastic compliances						
s_{11}	s_{12}	s_{13}	s_{15}	s_{22}	s_{23}	s_{25}
16·5	−2·75	−1·05	11·4	11·6	−4·41	−3·58
s_{33}	s_{35}	s_{44}	s_{46}	s_{55}	s_{66}	
9·05	4·19	49·9	−18·0	53·1	38·2	

summarizes the electrical resistivity values, together with the melting point values. Among them, we found an extraordinarily high conductivity value, 10^{-5} S cm^{-1}, compared with those of other organic semiconductors constructed from a single component. The cause of this high conductivity should result from the close packing of the molecule in the crystal. The central six atoms (the tetrathioethylene group) are coplanar, whereas the outer dithioethylene groups on each side form two other planes. The angle between the central plane and the outer planes decreases with increasing n, as shown in figure 9 from X-ray analysis data. Further, from the crystal structural data, the shortest distance between sulphur atoms of a C_6S_8 skeleton in two adjacent molecules was found to be 3·57 Å for TTC_9TTF and also for $TTC_{10}TTF$, which is considerably shorter than the sum of the van der Waals radii, 3·70 Å. On the other hand, the corresponding value for TTC_1TTF and TTC_2TTF is 3·80 Å. The proximity in TTC_nTTF, where n is larger than 6, is attributed to the strong interchain interaction between the two pairs of long paraffin chains (Wang *et al.* 1989), and in turn, is used to explain the high conductivity; the central skeleton has been 'fastened' together strongly with the four long alkyl chains. We call this type of organic semiconductor by the name *molecular fastener.*

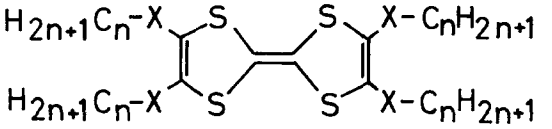

Figure 8. TXC_nTTF (X = S, Se and Te; n = 1–18). X = S is illustrated as TTC_nTTF.

Table 4. Electrical resistivity and melting point of TXC_nTTF (see figure 8). ρ values in parentheses are for compaction pellet specimens.

	S (TTC_nTTF)			Se ($TSeC_nTTF$)		Te ($TTeC_nTTF$)	
n	ρ (Ω cm)	m.p. (°C)		ρ (Ω cm)	m.p. (°C)	ρ (Ω cm)	m.p. (°C)
1	$2{\cdot}9 \times 10^{10}$	96·5	(L)	$1{\cdot}0 \times 10^{6}$	92·5	$8{\cdot}1 \times 10^{4}$	175·2
			(H)	$8{\cdot}5 \times 10^{7}$	106·3		
2	$1{\cdot}2 \times 10^{10}$	70·6		$3{\cdot}3 \times 10^{9}$	62·7	$2{\cdot}3 \times 10^{9}$	90·2
3	$9{\cdot}6 \times 10^{9}$	30·4		$6{\cdot}6 \times 10^{8}$	38·9	$7{\cdot}5 \times 10^{7}$	62·2
4	$6{\cdot}2 \times 10^{6}$	24·6		$1{\cdot}3 \times 10^{11}$	38·8	$1{\cdot}5 \times 10^{12}$	85·7
5	$6{\cdot}4 \times 10^{7}$	32·2		$3{\cdot}5 \times 10^{9}$	30·8	$2{\cdot}4 \times 10^{8}$	56·9
6	$3{\cdot}0 \times 10^{7}$	28·6		$1{\cdot}3 \times 10^{6}$	33·4	$6{\cdot}8 \times 10^{6}$	46·0
7	$3{\cdot}8 \times 10^{7}$	44·0		$9{\cdot}4 \times 10^{6}$	41·0	$5{\cdot}8 \times 10^{6}$	49·9
8	$7{\cdot}0 \times 10^{7}$	47·6		$7{\cdot}5 \times 10^{5}$	50·5	$1{\cdot}7 \times 10^{6}$	57·7
9	$5{\cdot}0 \times 10^{7}$	56·8		$(8{\cdot}3 \times 10^{5})$	56·5	$2{\cdot}0 \times 10^{6}$	65·2
10	$3{\cdot}7 \times 10^{5}$	59·4		$(1{\cdot}0 \times 10^{7})$	61·3		72·7
11	$5{\cdot}6 \times 10^{5}$	63·6		$(8{\cdot}4 \times 10^{6})$	65·6		77·7
12	$(5{\cdot}7 \times 10^{7})$	68·3		$(3{\cdot}8 \times 10^{6})$	75·0		82·2
13	$(2{\cdot}3 \times 10^{6})$	72·7		$(5{\cdot}6 \times 10^{6})$	79·7	$(1{\cdot}1 \times 10^{8})$	87·2
14	$(7{\cdot}8 \times 10^{7})$	76·5		$(6{\cdot}4 \times 10^{6})$	83·3	$(2{\cdot}6 \times 10^{8})$	89·2
15	$(2{\cdot}9 \times 10^{6})$	79·3		$(3{\cdot}3 \times 10^{6})$	85·2	$(1{\cdot}7 \times 10^{8})$	92·2
16	$(9{\cdot}9 \times 10^{6})$	83·3		$(2{\cdot}7 \times 10^{6})$	87·1	$(1{\cdot}2 \times 10^{8})$	94·2
17	$(1{\cdot}6 \times 10^{7})$	84·1		$(6{\cdot}3 \times 10^{6})$	90·0	$(1{\cdot}4 \times 10^{8})$	96·2
18	$(6{\cdot}8 \times 10^{9})$	85·0		$(3{\cdot}0 \times 10^{7})$	93·2	$(3{\cdot}5 \times 10^{8})$	97·5

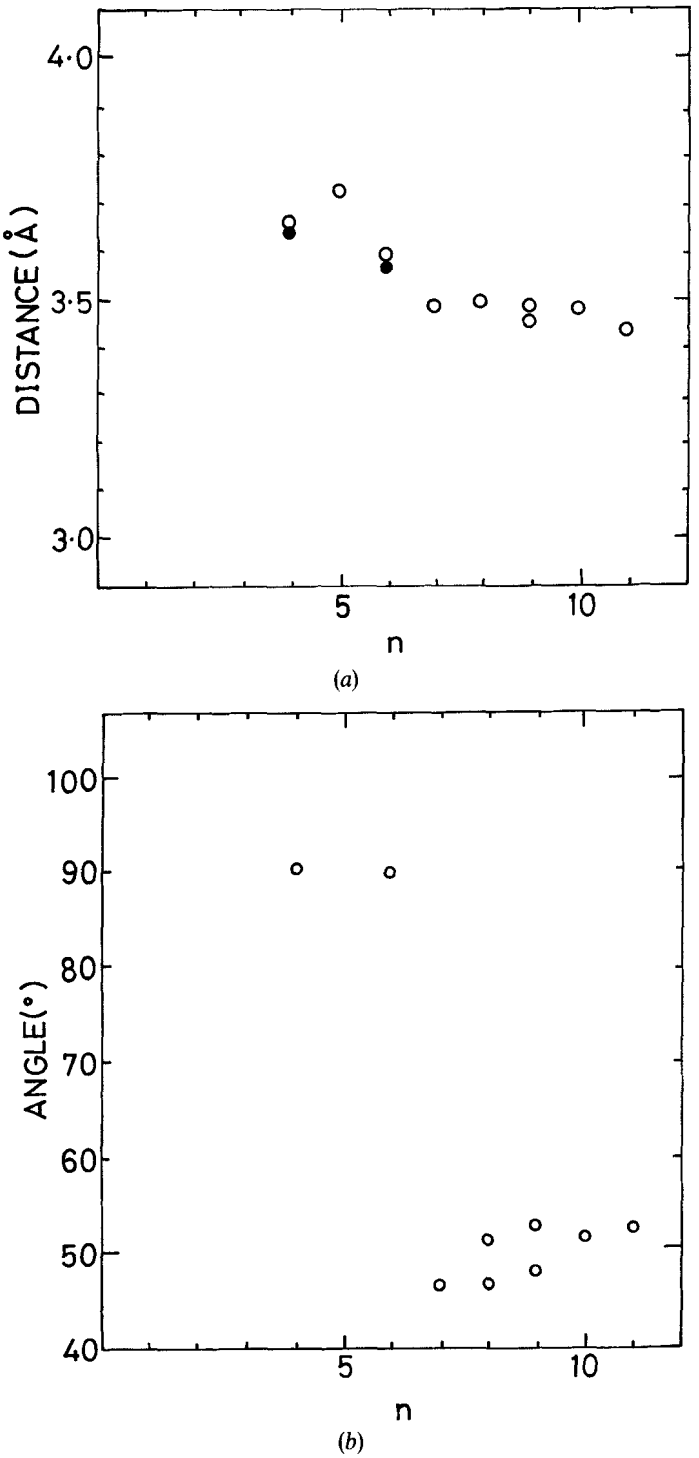

Figure 9. (*a*) The angle (in degrees) between the central plane and the outer plane of TTC_nTTF as function of n, (○), 24°C and (●), 0°C. (*b*) The shortest distance (Å) between S atoms of the C_6C_8 skeleton as a function of n.

This close-packing effect was confirmed by the measurement of ionization threshold energies: the energies were determined by the photoelectron spectroscopic method. It was notable that I_s and ρ (table 4) show a similar dependence on n as shown in figures 10 and 11 (Seki *et al.* 1986). The threshold ionization energy of isolated molecules remains constant within 0·1 eV. Therefore, the large variation among these compounds found in figure 10 is predominantly due to solid-state effects. The observed threshold energies of photoemission fall into two groups; $5{\cdot}0$–$5{\cdot}1_5$ eV for $n=1$ and 2, and $4{\cdot}7$–$4{\cdot}8_5$ eV for $n=8$–18. The latter values are outstandingly small for an organic solid, and are comparable to those for graphite. This condition usually implies ease of carrier generation, and might be a major reason for the high conductivity of these long-chain compounds. As already mentioned, the charge-carrier mobilities in organic solids are usually increased by applying external pressure (Kajiwara *et al.* 1967). The effect is caused by the broadening of the electronic band width due to the increase in intermolecular interaction. Internal pressure should be equally effective for producing this effect. In this system we propose that the 'molecular fastener effect' is a result of the internal pressure between molecules.

Mobility measurements for the TTC_nTTF series were carried out by Li and Maruyama. For TTC_9TTF needle-like crystals, the drift mobilities were observed at room temperature by using the surface-type time-of-flight method (Kamura *et al.* 1974). They were found to be quite high compared with ordinary values for organic molecular crystals; $\mu_{hole}=8{\cdot}7\pm1{\cdot}5\,cm^2\,V^{-1}\,s^{-1}$, and also $\mu_{electron}=19\pm4\,cm^2\,V^{-1}\,s^{-1}$ (see table 2). Recently, they also observed the temperature dependence of drift mobility of TTC_8TTF.

The series of TTC_nTTF crystals are known to show typical solid-state phase transitions. Among them, TTC_8TTF undergoes a crystal phase transition at 34°C and melts at 47·6°C. Around this solid–solid phase transition by decrease of temperature, a great jump of electrical resistivity occurred to a value approximately two degrees of magnitude higher.

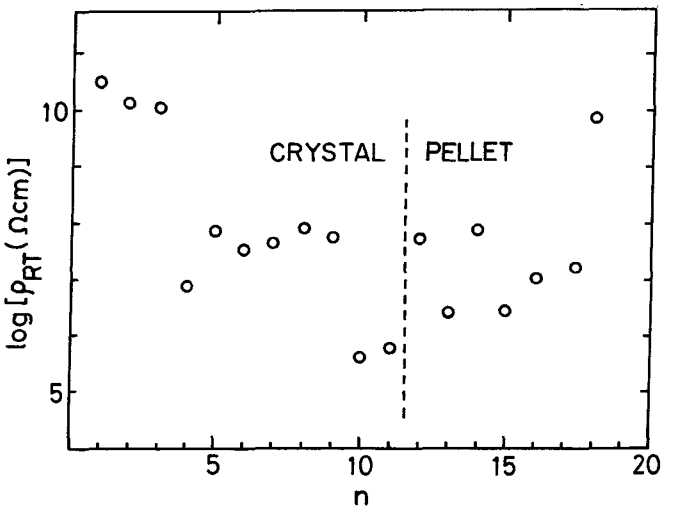

Figure 10. Dependence of electrical resistivity of TTC_nTTFs on the carbon number n in each alkyl chain.

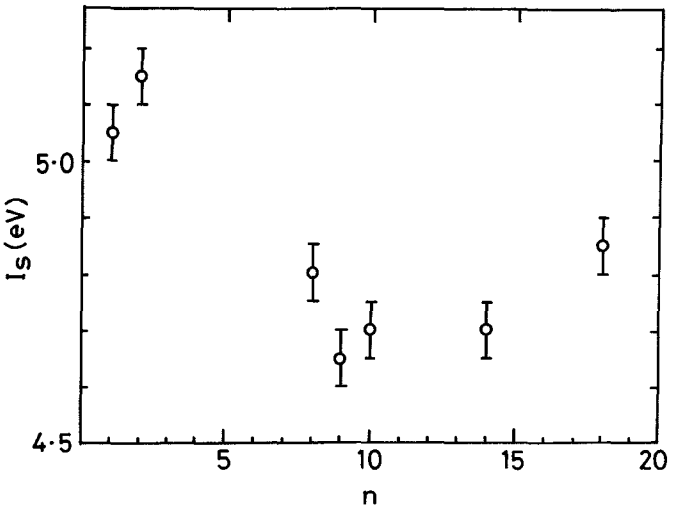

Figure 11. Dependence of ionization threshold energy I_s on n of figure 10.

The electron and hole mobilities at room temperature are 6·8 and 6·4 $cm^2 V^{-1} s^{-1}$ respectively. The temperature dependences of the charge mobility in the range of −100 to −45°C are summarized in table 5 and they are plotted against absolute temperature (T) in both logarithmic scales in figure 12.

From the slope in the low-temperature region (173–295 K), we can evaluate −1·8 for the negative exponent n in the relation of $\mu \propto T^n$:

$$\mu \propto T^{-1.8}.$$

This relation is consistent with data for usual organic crystals, $1 < n < 3$ as mentioned in the previous section. On the contrary, above 304 K, there exists a sharp drop in electron or hole mobility which corresponds to the resistivity jump at the solid–solid phase transition near 34°C. The resistivity jump is about two orders of magnitude as described above; thus we can conclude that the sharp reduction in mobility is predominantly responsible for the great jump in the electrical resistivity.

Table 5. Charge-carrier mobilities in a TTC_8TTF crystal as a function of temperature.

Temperature		Mobilities ($cm^2 V^{-1} s^{-1}$)	
t (°C)	T(K)	μ_{hole}	$\mu_{electron}$
−100	173	16·58	18·20
−72	201	11·88	12·22
−53	220	10·86	10·93
−25	248	7·75	8·41
0	273	6·72	7·59
22	295	6·40	6·78
31	304	4·34	6·01
37	310	1·93	2·54
45	318	0·77	1·33

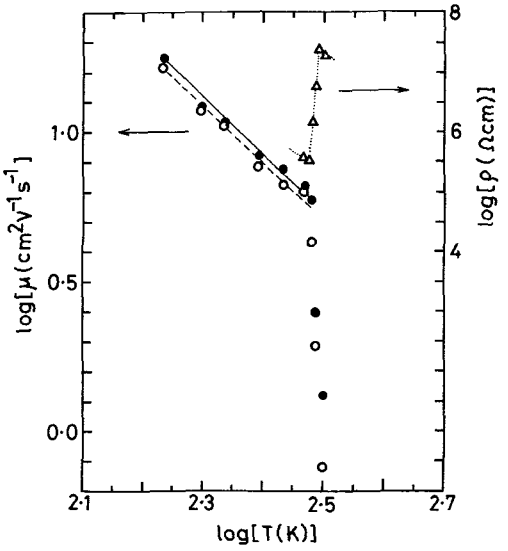

Figure 12. The carrier mobility of TTC_8TTF. Symbols correspond to data for holes (○) and electrons (●). The electrical resistivity is also indicated by open triangles.

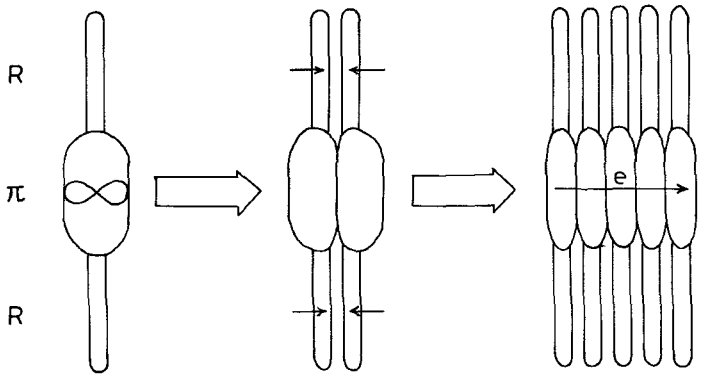

Figure 13. The molecular fastening principle.

These high mobilities, and also the low ionization threshold energy, have confirmed that the cause of the molecular fastener effect may be attributed to the following: the π electron system is at the centre of a molecule, with its plane perpendicular to the sheet, and the alkyl chains are attached to the both sides. When two molecules come together, the π systems are compressed by the attractive force between the alkyl chains. In the crystal, all the molecules come close to one another, and a strong overlap of π-orbitals is achieved; that is, the central π skeleton is strongly fastened by the long alkyl chains (figure 13).

5. Charge-transfer complexes

In 1954, we reported electrical conductivity of the perylene–bromine complex in *Nature* (Akamatu *et al.* 1954). The preparation of the complex, at that time, was reported by two groups; the complex was made by precipitation from a benzene solution of perylene by the addition of bromine (Brass and Clar 1932, 1936) and also by a direct absorption of bromine vapour by perylene (Zinke and Pongratz 1936, 1937). The specimens used in this study were prepared by the method of Zinke and Pongratz (Zinke and Pongratz 1936, 1937). The pressed pellets of the complex exhibited resistivities of about 8 Ω cm.

After that, we extended our work to the preparation of the complexes between polycyclic aromatic hydrocarbons and halogens, Br_2 and I_2 (Akamatu *et al.* 1956). Their electrical resistivities are listed in table 6. By these methods we were able to prepare stable complexes of violanthrene–iodine, and obtain reproducible findings of electrical resistivities. Since then a large number of investigations on conductive organic compounds have been reported.

In 1957, the electrical resistivities of semi-quinone type complexes with their catalytic activity were presented at the Third Conference on Carbon (Eley and Inokuchi 1959). In that conference, we reported the electrical resistivities of the organic–organic complexes of dimethyl aniline with chloranil, bromanil and iodanil, as listed in table 7. Further, we reported the a.c. and d.c. electrical resistivities of N,N-dimethyl aniline and tetramethyl-*p*-phenylene diamine complexes (Eley *et al.* 1959).

At the same time, Bijl *et al.* carried out measurements over the temperature range 293–263 K on the variation of d.c. resistance of pressed pellets of similar complexes (Bijl *et al.* 1959).

During the 1950s, as described above, a series of organic multicomponent semiconductors were established. As the study of the conductivity of such complexes progressed the term 'conducting charge-transfer complex' was applied to these conducting complexes. The term 'charge-transfer complex' is a fairly broad concept and means a substance formed by the interaction of two or more component molecules

Table 6. Semiconductivity data at room temperature of complex.

Complex (ratio)	ρ (Ω cm)	Temperature range (°C)		$\Delta\varepsilon$†
Perylene–bromine (1 : 4·4)	7·8	−20	−170	0·13
Pyranthrene–bromine (1 : 3·3)	220	−20	−170	0·20
Violanthrene–bromine (1 : 4·5)	66	−20	−170	0·20
Violanthrene–iodine (1 : 4·0)	45	−20	−170	0·15
Violanthrene–iodine (1 : 4·0)	45	10	60	0·14

† $\rho = \rho_0 \exp(\Delta\varepsilon/2kT)$.

Table 7. Semiconductivity ρ (Ω cm) of semiquinone-type complexes.

Donor	N,N-dimethyl aniline		
Acceptor	Chloranil	Bromanil	Iodanil
a.c.	$5{\cdot}0 \times 10^7$	$9{\cdot}0 \times 10^7$	$3{\cdot}0 \times 10^7$
d.c.	$8{\cdot}0 \times 10^8$	$1{\cdot}5 \times 10^9$	$1{\cdot}7 \times 10^8$

or ions, the presence of which may be recognized by its colour (Matsunaga 1989). When we use a strong acceptor, for instance bromine, it appears that the complexes are largely ionic; most of them may be regarded as ion-radical salts, and they are called charge-transfer salts. Among these salts, those with compositions different from 1 : 1, that is to say in which both neutral and charged molecules of the donor or acceptor compound exist, tend to exhibit resistivity much lower than the corresponding 1 : 1 salts. Consequently, ion-radical salts are considered as *mixed-valence* compounds. In section 6, we show that organic superconductors can also be regarded as mixed-valence compounds.

From these concepts of 'complex' formation, the selection of suitable 'donors' and 'acceptors' is the major task in order to produce a variety of electrical conduction values, from semiconduction to superconduction.

Generally speaking, when the ionization energy (I_D; corresponding to I_a of section 2) of the donor is low, and the electron affinity (E_A) of the acceptor molecule is high, the resulting complex tends to be ionic. The formation of a charge-transfer salt is governed not only by the energy needed to charge the molecules, but also by the electrostatic energy of the ionic lattice. The electrostatic energy, as mentioned in section 2, depends on the packing of the component ions, which in turn depends on the molecular size and shape of the donor and acceptor. As functions of I_D and E_A, Matsunaga has made a map of the conductive complex region (figure 14) (Matsunaga 1969). He arranged the complexes on a chart, placing I_D on the abscissa and E_A on the ordinate. In this map, lines with a slope of -1 become the scale for I_D–E_A. This map shows how the electrostatic energy can vary with the kinds of component molecules.

In this map, X, the energy of the charge-transfer absorption maximum in the *s*-trinitrobenzene complex in a chloroform solution, is taken as a measure of I_D. Y, charge transfer band in the pyrene complex, is taken as a measure of E_A. Then, the complex on the line of $Y = -X +$ constant exhibits charge-transfer absorption at nearly the same energy. For example in the figure, the upper line corresponds to the energy of $15 \times 10^3\ cm^{-1}$, and the lower one to $10 \times 10^3\ cm^{-1}$.

As donors, six amines are listed in the figure: **(I)** N,N,N′,N′-tetramethyl-*p*-phenylenediamine (TMPD), **(II)** 1,6-diaminopyrene, **(III)** N,N,N′,N′-tetramethylbenzidine, **(IV)** diaminodurene, **(V)** 1,5-diaminonaphthalene and **(VI)** *p*-phenylenediamine. The acceptors employed as standard compounds are: (*a*) 2,3-dichloro-5,6-dicyano-*p*-benzoquinone (DDQ), (*b*) tetracyano-*p*-benzoquinodimethane (TCNQ), (*c*) tetracyanoethylene (TCNE), (*d*) 2,3-dicyano-1,4-naphthoquinone, (*e*) 9-dicyanomethylene-2,4,7-trinitrofluorene, (*f*) *p*-chloranil, (*g*) *p*-fluoranil, (*h*) 2,5-dichlor-*p*-benzoquinone, (*i*) 2,4,7-trinitrofluorenone and (*j*) dichloro-*p*-xyloquinone. In this map, the open circles indicate non-ionic complexes and the shaded circles ionic complexes. The complexes which exist in the region where both X and Y have large values are non-ionic, and those in the opposite region are ionic. We found several exceptions which reflect the effects of molecular size and shape on their electronic structures. However, using this map, we have a guiding principle to search for conductive charge-transfer complexes. The discovery of TCNQ as a π acceptor and tetrathiafulvalene (TTF) (Wudl *et al.* 1970) had a major influence on the search for conductive charge-transfer complexes. The group at Johns Hopkins University found that single crystals of the TTFTCNQ complex showed metal-like electrical conductivity (Cohen *et al.* 1973, Coleman *et al.* 1973). The finding of metallic character in organic solids led rapidly to the discovery of superconduction in organic material in the low-temperature region (see section 6).

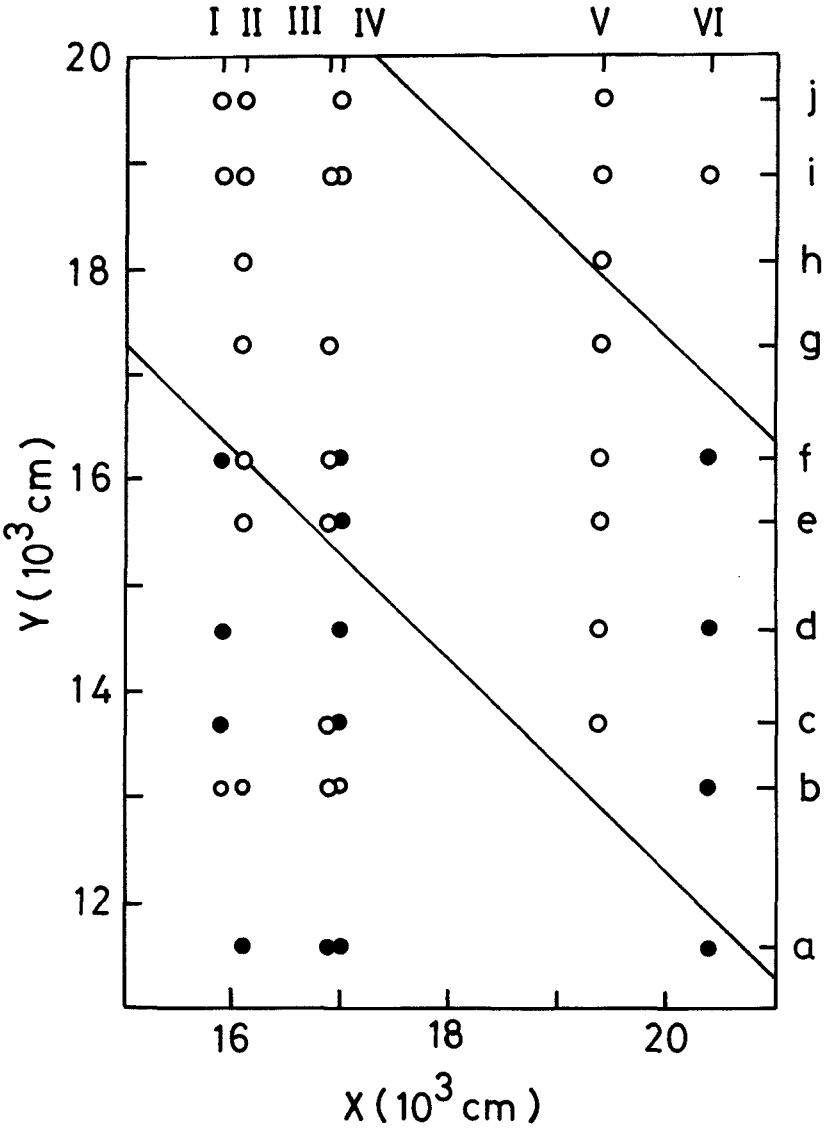

Figure 14. Electronic structures of molecular complexes as revealed by the vibrational spectra. The non-ionic complexes are indicated by open circles and the largely ionic complexes by shaded circles.

5.1. *Catalytic activity of charge-transfer complexes*

Departing from the subject of this review, the authors wish to describe briefly the catalytic activity of these charge-transfer complexes.

Our first report on this subject appeared in the Proceedings of the Third Conference on Carbons (Eley and Inokuchi 1959). We studied the applied $H_2 + D_2 \leftrightarrows 2HD$ reaction on semiquinone-type complexes, but no trace of reaction could be found.

In 1965, we prepared a highly photoemissive charge transfer complex, tetracyanopyrene–Cs (Ogino *et al.* 1965). We found a definite $H_2 + D_2 \leftrightarrows 2HD$ reaction for this complex (Kondow *et al.* 1965). We applied this catalytic reaction to several other aromatic–alkali metal charge-transfer complexes and also graphite intercalation compounds (Inokuchi *et al.* 1967). Table 8 summarizes their activities. The mechanism of this activity can be explained by the dissociation of molecular hydrogen to combine with the alkali metal atom. This work has been extended to hydrogen–alkali-metal–graphite ternary intercalation compounds (Enoki *et al.* 1990) and also electrical conduction in cytochrome c_3 solid (Yagi *et al.* 1983).

6. Organic superconductors

The first report of the discovery of an organic superconductor, tetramethyltetraselenafulvalenium cation radical salt, $(TMTSF)_2PF_6$, appeared in 1980 (Jerome *et al.* 1980). Since then, major efforts to discover new organic superconductors have been successful for thirty different charge-transfer complexes. Table 9 summarizes their structures and also the transition temperatures (Inokuchi 1988). We have contributed to this field of organic superconductors by the preparation of the electron donor molecule, alkylthio-substituted tetrathiafulvalene (TTF), and by the discovery of several organic superconductors. The alkylthio-substituted TTF, BEDTTTF (figure 15), was made in the hope that the chemical modification of extending the TTF moiety, with an increased polarizability, would increase the conduction band width and reduce the on-site Coulomb repulsion, resulting in a considerable enhancement of the metallic character (Saito *et al.* 1982).

Using this π donor, single crystals of the organic cation radical salt, BEDT–TTF.ClO_4 with solvent, were prepared by the electrocrystallization technique. In figure 16, the resistivity data is depicted along the elongated direction of the crystal, which is close to the *a* axis in the *a*–*c* plane. The resistivity decreases monotonically from the room temperature value ($\rho_{RT} = 3{\cdot}8 \times 10^{-2}\,\Omega$ cm) to a minimum at 16 K, T_{min}. ($\rho_{min} = 1{\cdot}0 \times 10^{-3}\,\Omega$ cm). Then it increased very gradually down to the lowest measured temperature (1·4 K) where the resistivity is well below the room temperature value. The magnitude of the resistivity varies from sample to sample, but the ratio ρ_{RT}/ρ_{min} and the T_{min} value are almost constant at 35 ± 3 and 16 ± 1 K. Also in figure 16, the temperature dependency of $(TMTTF)_2ClO_4$ along the stacking axis is taken from Delhaes' work (Delhaes *et al.* 1979). This comparison suggests that the BEDT–TTF salt has stronger

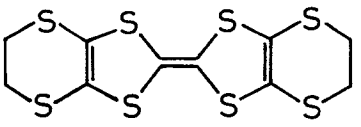

Figure 15. BEDT–TTF.

Table 8. The conversion and the exchange of hydrogen with the charge-transfer complexes.

Complex				
Donor	Acceptor	p-$H_2 \rightleftharpoons o$-H_2	$H_2 + D_2 \rightleftharpoons 2HD$	$H_2 \rightleftharpoons D_2$
Cs	Tetracyanopyrene	[195–373 K]† Occurred $E = 3{\cdot}7$ kcal mol^{-1} Proceeded at 77 K	[273–373 K] Proceeded at a comparable rate with p-$H_2 \rightleftharpoons o$-H_2 none at 77 K	—
Cs	Tetranitropyrene	...	[273–373 K] None	—
Na	Tetracyanoethylene	[273–373 K] Very slow conversion	[273–373 K] None	—
Na	Phthalonitrile	[273–373 K] Occurred $E = 4{\cdot}4$ kcal mol^{-1}	[273–373 K] Proceeded at a comparable rate with p-$H_2 \rightleftharpoons o$-H_2	[273–373 K] Slow reaction $E = 17$ kcal mol^{-1}
Na	Terephthalonitrile	[273–383 K] Scarcely occurred at a measureable rate	(273–373 K] Scarcely occurred at a measureable rate	(273–373 K] None
Cs	Violanthrene B	[273–423 K] Occurred strongly $E = 10{\cdot}0$ kcal mol^{-1}	[273–423 K] Occurred	[273–423 K] Proceeded $E \simeq 17{\cdot}2$ kcal mol^{-1}
Cs	Graphite	[195–301 K] Occurred strongly $E = 0{\cdot}6$ kcal mol^{-1}	[195–301 K] Proceeded at a comparable rate with p-$H_2 \rightleftharpoons o$-H_2	—

† Values in brackets indicate temperature range of observation.

Table. 9 Organic superconductors (Inokuchi 1988).

Compounds	T_c
$(TMTSF)_2PF_6$	1·4 K (6·5 kbar)
$(TMTSF)_2AsF_6$	1·4 K (9·5 kbar)
$(TMTSF)_2SbF_6$	0·38 K (10·5 kbar)
$(TMTSF)_2TaF_6$	1·35 K (11 kbar)
$(TMTSF)_2ClO_4$	1·4 K
$(TMTSF)_2ReO_4$	1·2 K (9·5 kbar)
$(TMTSF)_2FSO_3$	2·1 K (6·5 kbar)
$(BEDT\text{–}TTF)_2ReO_4$	2 K (4 kbar)
β-$(BEDT\text{–}TTF)_2I_3$	1·5 K
	8 K (1·3 kbar)
β-$(BEDT\text{–}TTF)_2IBr_2$	2·5 K
β-$(BEDT\text{–}TTF)_2AuI_2$	3·8–5 K
γ-$(BEDT\text{–}TTF)_2(I_3)_{2\cdot5}$	2·5 K
θ-$(BEDT\text{–}TTF)_2I_3$	3·6 K
κ-$(BEDT\text{–}TTF)_2I_3$	3·6 K
$(BEDT\text{–}TTF)_4Hg_3Cl_8$	1·8 K (12 kbar)
$(BEDT\text{–}TTF)_4Hg_3Br_8$	4·3 K
$(BEDT\text{–}TTF)_3Cl_2(H_2O)_2$	2 K (16 kbar)
$(BEDT\text{–}TTF)_2Cu(NCS)_2$	10·4 K
TTF[Ni(dmit)$_2$]$_2$[a]	1·6 K (7 kbar)
α-TTF[Pd(dmit)$_2$]$_2$[a]	6 K (19 kbar)
$[(CH_3)_4$[Ni(dmit)$_2$]][a]	5 K (7 kbar)
$(DMET)_2Au(CN)_2$[b]	0·8 K (5 kbar)
$(DMET)_2AuCl_2$[b]	0·83 K
$(DMET)_2AuI_2$[b]	0·55 K (5 kbar)
$(DMET)_2I_3$[b]	0·47 K
$(DMET)_2IBr_2$[b]	0·59 K
$(DMET)_2AuBr_2$[b]	1 K (1·5 kbar)
$(MDT\text{–}TTF)_2AuI_2$[c]	3·5 K

[a] [Ni(dmit)$_2$] =

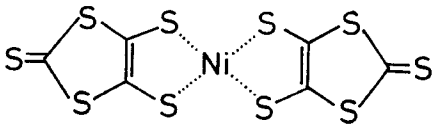

[b] DMET =

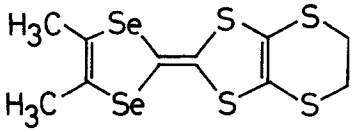

[c] MDT–TTF =

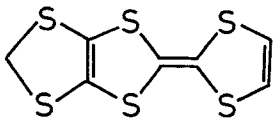

metallic character than the TMTTF salt. An anisotropy study of electrical resistivity has found that the BEDT–TTF salt is almost two-dimensional rather than one-dimensional, as usually observed in organic metals. The anisotropical value, $\rho_{//}/\rho_{\perp}$, where $\rho_{//}$ is along the elongated direction and $\rho_{\perp}$ is normal to it in the *a–c* plane, is 0·9 at room temperature and decreases slightly to 0·4 at 3 K. On the other hand, the resistivity along the direction normal to the *a–c* plane is 10^2–10^3 times bigger than ρ at room temperature. From these experimental observations, we concluded that the BEDT–TTF salt shows two-dimensional transport properties in the *a–c* plane over the entire temperature range measured. This two-dimensional character was confirmed from the crystal structure analysis (Kobayashi *et al.* 1983).

From these results of the two-dimensional character of the electrical, optical and also structural data, we have proposed practical molecular designs for organic metals with strong interchain interaction, which become organic superconductors of the $(TMTSF)_2X$ type.

In 1983, the BEDT–TTF salt, $(BEDT\text{–}TTF)_2ReO_4$, was the first organic superconductor found in the BEDT–TTF series (Parkin *et al.* 1983). As listed in table 9, two-thirds of organic superconductors are BEDT–TTF derivatives; that is to say, at present, BEDT–TTF is the most appropriate π donor to produce organic superconductors. Among them, two sorts of superconducting BEDT–TTF salts were prepared in our group; one of them includes the chemically active element Cl_2 and the other is the first organic superconductor with a T_c higher than 10 K under ambient pressure.

6.1. *(BEDT–TTF)$_3$Cl$_2$.2H$_2$O (Mori and Inokuchi 1987a)*

The chlorine salt $(BEDT\text{–}TTF)_3Cl_2.2H_2O$ shows superconduction at 2 K under a pressure of 16 kbar. The black plate-like crystals were grown by electrochemical crystallization of BEDT–TTF in benzonitrile with $[(C_2H_5)_4N]_2CoCl_4.xH_2O$ as a supporting electrolyte (Mori and Inokuchi 1987b). An enormous number of charge-transfer complexes with halogens as acceptors have been prepared. However, no report of complex formation with chlorine has appeared as far as we know. From the viewpoint of the structural chemistry of BEDT–TTF salts, the discontinuity between iodine and bromine is related to the ability of iodine to form trimer anions such as I_3^-. On the other hand, Br and Cl atoms are themselves too small to form charge-transfer complexes with BEDT–TTF, but the clusters solvated by H_2O are included in the BEDT–TTF salts.

The 3 : 2 BEDT–TTF salts occur when the counter-anions are relatively small, such as with ClO_4^- and ReO_4^-. The Br and Cl salts not only have the same composition but also a similar donor arrangement as the salts of these tetrahedral anions. The complex anion clusters, $Br_2(H_2O)_2$ and $Cl_4(H_2O)_4$, can be regarded as rather small anions.

The structure of the anion $Cl_4(H_2O)_4$ in the salt is illustrated in figure 17. Two chlorine atoms are connected to two oxygen atoms through hydrogen bonds to form a rectangle. This unit has a close resemblance to the $Br_2(H_2O)_2$ unit in $(BEDT\text{–}TTF)_3Br_2(H_2O)_2$. However, in the chlorine salts additional Cl and O atoms are attached to this unit by hydrogen bonding.

The bromine salt, $(BEDT\text{–}TTF)_3Br_2(H_2O)_2$, exhibits metallic conduction at room temperature, and then undergoes a metal-to-insulator transition at 185 K. The chlorine salt $(BEDT\text{–}TTF)_3Cl_2.2H_2O$ has a high conductivity, 500 S cm^{-1}, at room temperature and exhibits metallic behaviour down to 100 K. Although this chlorine

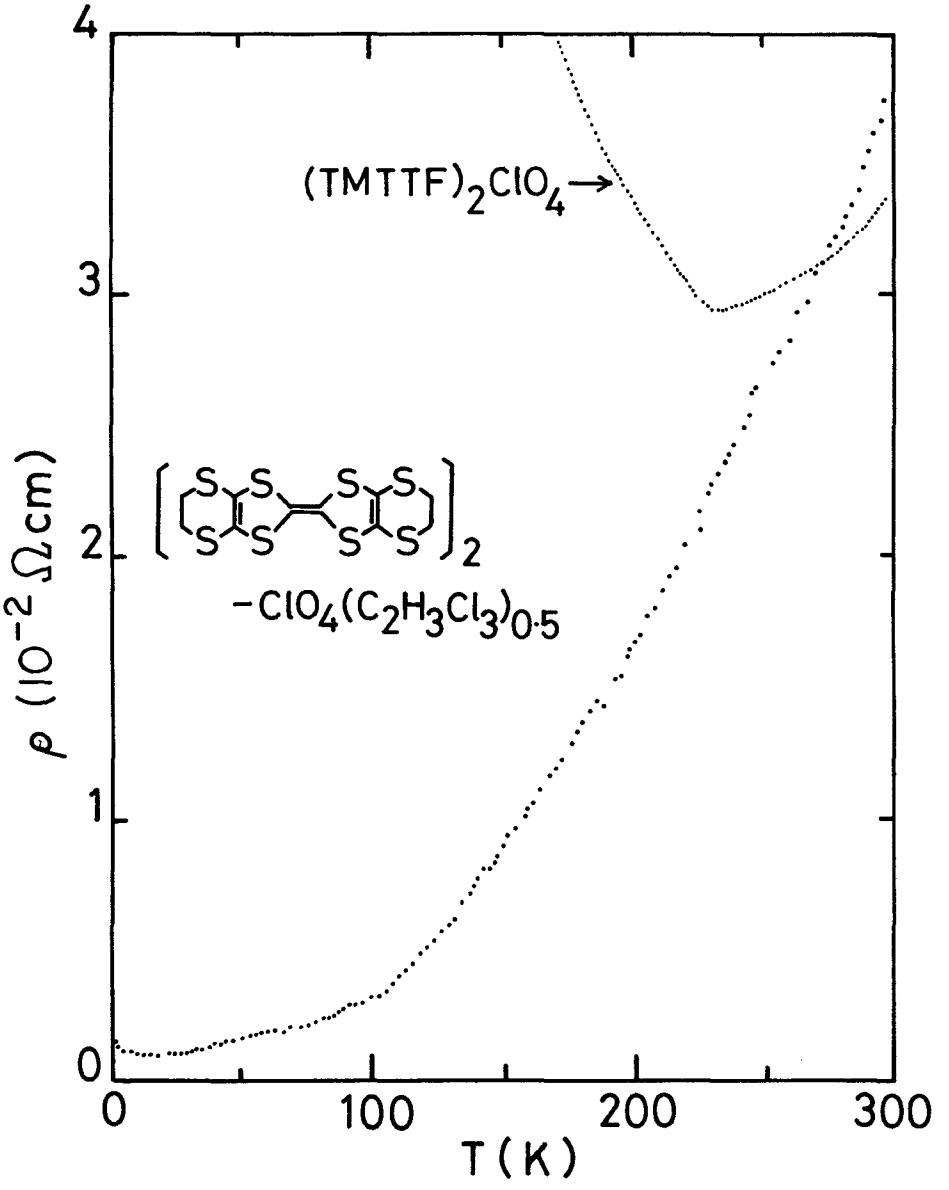

Figure 16. Electrical resistivity against temperature along the elongated axis of a (BEDT–TTF)$_2$ClO$_4$.(1,1,2-trichloroethane)$_{0.5}$ single crystal. Also shown is that of (TMTTF)$_2$ClO$_4$ along the stacking axis.

salt undergoes a metal-to-insulator transition around 100 K, superconductivity has been found at 2 K under pressure of 16 kbar, as mentioned above.

Apart from the superconducting behaviour of this chlorine salt, the structure of the anion $[Cl_4(H_2O)_4]^-$ is quite an unusual one. In the future, we may use these complex ions to synthesize new types of compounds such as $[Cl_4(H_2O)_4]^-$.

6.2. *(BEDT–TTF)$_2$Cu(NCS)$_2$ (Urayama* et al. *1988a, b)*

This salt is a superconductor with $T_c = 10{\cdot}4$ K under ambient pressure. The crystal structure of $(BEDT–TTF)_2Cu(NCS)_2$ is analagous to that of κ-$(BEDT–TTF)_2I_3$. Two BEDT–TTF molecules form a pair, and the pairs are linked to each other by S···S contacts almost perpendicularly, building two-dimensional conducting sheets in the *b–c* plane. Each conducting layer is sandwiched by the insulating layers of anions along the *a* axis. The anion $Cu(NCS)_2$ is asymmetric, bent like a boomerang. The boomerang

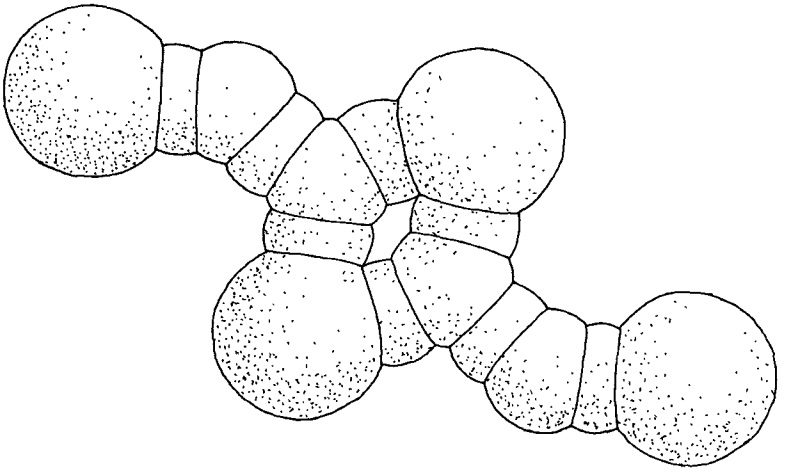

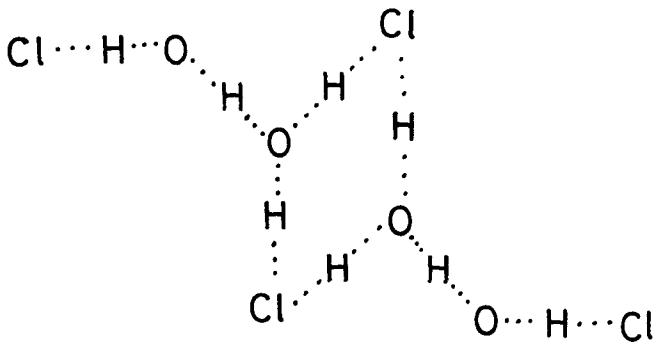

Figure 17. Structural model of the $Cl_4(H_2O)_4^-$ anion.

units are arranged one after the other along the *b* axis to form a zig-zag one-dimensional flat polymer. Three NCS groups coordinate to a copper cation (Cu^+) via two nitrogen atoms and one sulphur atom. The one-dimensional polymer can thus be represented as

$$\begin{array}{c}(\text{–SCN–Cu–})_n \\ \quad\quad | \\ \quad\quad \text{NCS}\end{array}$$

in which structure two isomers, thiocyanate and isothiocyanate, are coordinated to a copper cation. This unusual structure suggests that a peculiar force in the charge-transfer complex strongly influences the formation of new types of chemical species.

Figure 18 shows the electrical resistivity (ρ) of $(BEDT\text{–}TTF)_2Cu(NCS)_2$ as a function of temperature. The ρ value at room temperature along the crystal long axis (the *b* axis) was $2\text{–}7 \times 10^{-2}\,\Omega\,cm$. In the *b–c* plane the resistivity is almost isotropic, while along the *a* axis the resistivity is 600 to 1000 times larger than that in the *b–c* plane. As illustrated in figure 18, down to 270 K weak metallic behaviour was observed. Therefore, the resistivity increases with decreasing temperature, and the maximum value at around 90 to 100 K is four to six times greater than that at room temperature, and below 90 K metallic behaviour reappeared followed by a superconducting transition at 10·4 K. Maruyama *et al.* (1988) observed the tunnelling current characteristics of $(BEDT\text{–}TTF)_2Cu(NCS)_2$ by means of tunnelling spectroscopy. From those data, the observed gap of 4 meV leads to a value of 4·5 for $2\Delta/kT_c$ ($2\Delta = 4$ meV and $T_c = 10{\cdot}4$ K), which is of the same order as the Bardeen–Cooper–Schrieffer (BCS) ratio of 3·52.

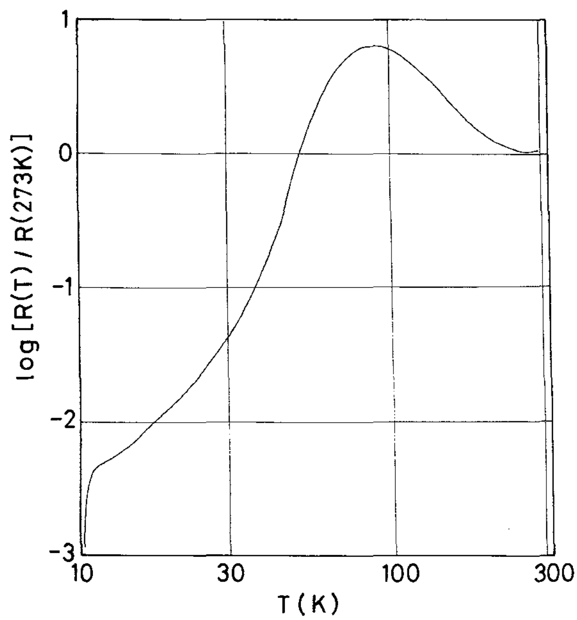

Figure 18. Temperature dependendence of the electrical resistivity of the complex $(BEDT\text{–}TTF)_2Cu(NCS)_2$.

6.3. *Superconduction of graphite intercalates*

Graphite, of course, is not an organic compound. However we can *consider* that graphite is the largest polycyclic aromatic compound, as mentioned previously. From such a viewpoint, we present here the superconductivity of graphite intercalates. Graphite forms intercalation compounds with alkali metals easily. Their compositions are C_8M and $C_{12n}M$ ($n \geqslant 2$; M = K, Rb and Cs). Among those, in C_8M, the first stage compound, the layers of hexagonally-arrayed carbon atoms and alkali metals are stacked alternately.

The first report of superconduction of C_8M appeared in 1965 (Hannay *et al.* 1965), but without detailed superconducting properties. Thereafter, several articles on superconductivity of C_8K were published; the superconducting transition temperatures (T_c) are 0·39 K for a stochiometric compound C_8K obtained from pyrolytic graphite (Hannay *et al.* 1965), 0·55 K for a compound made with excess potassium (Hannay *et al.* 1965), 0·139 K for a pseudo-single crystal of C_8K (Koike *et al.* 1978), 0·125 K for $C_{8\cdot8}K$ obtained from grafoil (Kobayashi and Tsujikawa 1979), and 0·080 K for a $C_{8\cdot07}K$ powder sample (Kobayashi and Tsujikawa 1977).

In 1980, using the grafoil–K intercalation compound, the superconducting transition temperature T_c was detected by measuring the temperature dependence of the a.c. magnetic susceptibility χ in a low magnetic field; $T_c = 0{\cdot}126$ K for $C_{8\cdot6}K$ and $T_c = 0{\cdot}108$ K for $C_{10}K$ (Sano *et al.* 1980).

More accurate observations were carried out with highly oriented pyrolytic graphite reacted with Rb metal, $C_{7\cdot96}Rb$ (Kobayashi *et al.* 1985): we found that $C_{7\cdot96}Pb$ underwent a definite superconducting transition at $T_c = 26$ mK to become a type-I superconductor.

As illustrated in table 9, at the present time, very few π donors and one π acceptor can be conveniently used as components of charge-transfer type organic superconductors. Intensive searches to find appropriate donors and acceptors for producing good organic superconductors are desirable.

References

AKAMATU, H., and INOKUCHI, H., 1950, *J. chem. Phys.*, **18,** 810; 1952, *J. chem. Phys.*, **20,** 1481.

AKAMATU, H., INOKUCHI, H., and MATSUNAGA, Y., 1954, *Nature*, **173,** 168; 1956, *Bull. chem. Soc. Japan*, **29,** 213.

AKAMATU, H., INOKUCHI, H., TAKAHASHI, H., and MATSUNAGA, Y., 1956, *Bull. chem. Soc. Japan*, **29,** 574.

AKAMATU, H., and NAGAMATSU, K., 1947, *J. Colloid. Sci.*, **2,** 539.

BIJL, D., KAINER, H., and ROSE-INNES, A. C., 1959, *J. chem. Phys.*, **30,** 765.

BRASS, K., and CLAR, E., 1932, *Ber. deutsch. chem. Gesell.*, **65,** 1660; 1936, *Ibid.*, **69,** 1977.

COHEN, M. J., COWAN, L. B., WALATKA, V. JR, and PERLSTEIN, J. H., 1973, *J. Am. chem. Soc.*, **95,** 948.

COLEMAN, L. B., COHEN, M. J., SANDMAN, D. J., YAMAGISHI, F. G., GARITO, A. F., and HEEGER, A. J., 1973, *Solid-St. Commun.*, **12,** 1125.

DANNO, T., and INOKUCHI, H., 1968, *Bull. chem. Soc. Japan*, **41,** 1783.

DELHAES, P., COULON, C., AMIELL, J., FRANDROIS, S., TORIELLES, E., FABRE, J. M., and GIRAL, L., 1979, *Molec. Crystals liq. Crystals*, **50,** 43.

ELEY, D. D., 1948, *Nature*, **162,** 819.

ELEY, D. D., and INOKUCHI, H., 1959, *Proceedings of the Third Conference on Carbon*, edited by S. Mrozowski (Oxford: Pergamon), p. 91.

ELEY, D. D., INOKUCHI, H., and WILLIS, M. R., 1959, *Discuss. Faraday Soc.*, **28,** 54.

ENOKI, T., MIYAJIMA, S., SANO, M., and INOKUCHI, H., 1990, *J. Mater. Sci.* (to be published).

HANNAY, N. B., GEBALLE, T. H., MATTHIAS, B. T., ANDRES, K., SCHMIDT, P., and MACNAIR, D., 1965, *Phys. Rev. Lett.*, **14,** 225.

HARADA, Y., and INOKUCHI, H., 1966, *Bull. chem. Soc. Japan*, **39,** 1443.
HIROOKA, T., TANAKA, K., KUCHITSU, K., FUJIHIRA, M., INOKUCHI, H., and HARADA, Y., 1973, *Chem. Phys. Lett.*, **18,** 390.
HOLSTEIN, T., 1959 a, *Ann. Phys.*, **8,** 325; 1959 b, *Ibid.*, **8,** 343.
INOKUCHI, H., 1951, *Bull. chem. Soc. Japan*, **24,** 222; 1954, *Ibid.*, **27,** 22; 1971, *Discuss. Faraday Soc.*, **51,** 183; 1988, *Angew. Chem.*, **100,** 1817.
INOKUCHI, H., and HARADA, Y., 1963, *Nature*, **198,** 477.
INOKUCHI, H., IMAEDA, K., ENOKI, T., MORI, T., MARUYAMA, Y., SAITO, G., OKADA, N., YAMOCHI, H., SEKI, K., HIGUCHI, Y., and YASUOKA, N., 1987, *Nature*, **329,** 39.
INOKUCHI, H., SAITO, G., WU, P., SEKI, K., TANG, T. B., MORI, T., IMAEDA, K., ENOKI, T., HIGUCHI, Y., INABA, K., and YASUOKA, N., 1986, *Chem. Lett.*, 1263.
INOKUCHI, H., SEKI, K., and SATO, N., 1987, *Physica Scripta T*, **17,** 93.
INOKUCHI, H., WAKAYAMA, N., KONDOW, T., and MORI, Y., 1967, *J. chem. Phys.*, **46,** 837.
JEROME, D., MAZAUD, A., RIBAULT, M., BECHGAARD, K., 1980, *J. Phys.*, **41,** L95.
KAJIWARA, T., INOKUCHI, H., and MINOMURA, S., 1967, *Bull. chem. Soc. Japan*, **40,** 1055.
KAMURA, Y., INOKUCHI, H., and MARUYAMA, Y., 1974, *Chem. Lett.*, 301.
KEPLER, R. G., 1960, *Phys. Rev.*, **119,** 1226.
KOBAYASHI, H., KOBAYASHI, A., SASAKI, Y., SAITO, G., ENOKI, T., and INOKUCHI, H., 1983, *J. Am. chem. Soc.*, **105,** 297.
KOBAYASHI, K., and BROWN, F. C., 1959, *Phys. Rev.*, **133,** 507.
KOBAYASHI, M., ENOKI, T., INOKUCHI, H., SANO, M., SUMIYAMA, A., ODA, Y., and NAGANO, H., 1985, *J. Phys. Soc. Japan*, **54,** 2359.
KOBAYASHI, M., and TSUJIKAWA, T., 1977, *National Meeting of The Physical Society of Japan.*
KOBAYASHI, M., and TSUJIKAWA, I., 1979, *J. phys. Soc. Japan*, **46,** 1945.
KOCHI, M., HARADA, Y., HIROOKA, T., and INOKUCHI, H., 1970, *Bull. chem. Soc. Japan*, **43,** 2690.
KOIKE, Y., SUEMATSU, H., HIGUCHI, K., and TANUMA, S., 1978, *Solid-St. Commun.*, **27,** 623.
KONDOW, T., INOKUCHI, H., and WAKAYAMA, N., 1965, *J. chem. Phys.*, **43,** 3766.
LEBLANC, O. H. JR, 1960, *J. chem. Phys.*, **33,** 626.
MARUYAMA, Y., 1989, *Molec. Crystals liq. Crystals*, **171,** 287.
MARUYAMA, Y., INABE, T., URAYAMA, H., YAMOCHI, H., and SAITO, G., 1988, *Solid-St. Commun.*, **67,** 35.
MARUYAMA, Y., and INOKUCHI, H., 1967, *Bull. chem. Soc. Japan*, **40,** 2073.
MATSUNAGA, Y., 1969, *Bull. chem. Soc. Japan*, **42,** 4290; 1989, *Molec. Crystals liq. Crystals*, **171,** 193.
MORI, T., and INOKUCHI, H., 1987a, *Chem. Lett.*, 1657; 1987b, *Solid-St. Commun*, **64,** 335.
OGINO, K., IWASHIMA, S., INOKUCHI, H., and HARADA, Y., 1965, *Bull. chem. Soc. Japan*, **38,** 473.
PARKIN, S. S. P., ENGLER, E. M., SCHUMAKER, R. R., LATIER, R., LEE, V. Y., SCOTT, J. C., and GREENE, R. L., 1983, *Phys. Rev. Lett.*, **50,** 270.
REDFIELD, A. G., 1954, *Phys. Rev.*, **94,** 526, 537.
SAITO, G., ENOKI, T., TORIUMI, K., and INOKUCHI, H., 1982, *Solid-St. Commun.*, **42,** 557.
SANO, M., INOKUCHI, H., KOBAYASHI, M., KANEIWA, S., and TSUJIKAWA, I., 1980, *J. chem. Phys.*, **72,** 3840.
SATO, N., SEKI, K., and INOKUCHI, H., 1981, *J. chem. Soc. Faraday Trans.* II, **77,** 1621.
SCHEIN, L. B., and BROWN, D. W., 1982, *Molec. Crystals liq. Crystals*, **87,** 1.
SEKI, K., INOKUCHI, H., HARADA, Y., 1973, *Chem. Phys. Lett.*, **20,** 197.
SEKI, K., TANG, T. B., MORI, T., WU, P., SAITO, G., and INOKUCHI, H., 1986, *J. chem. Soc. Faraday Trans.* II, **82,** 1067.
URAYAMA, H., YAMOCHI, H., SAITO, G., SATO, S., KAWAMOTO, A., TANAKA, J., MORI, T., MARUYAMA, Y., and INOKUCHI, H., 1988a, *Chem. Lett.*, 463.
URAYAMA, H., YAMOCHI, H., SAITO, G., NOZAWA, K., SUGANO, T., KINOSHITA, M., SATO, S., OSHIMA, K., KAWAMOTO, A., TANAKA, J., 1988b, *Chem. Lett.*, 55.
VARTANYAN, A. T., 1948, *Zh. fiz. Khim.*, **22,** 769.
WANG, P., ENOKI, T., IMAEDA, K., IWASAWA, N., YAMOCHI, H., URAYAMA, H., SAITO, G., and INOKUCHI, H., 1989, *J. phys. Chem.*, **93,** 5947.
WUDL, F., SMITH, G. M., and HUFNAGEL, E. J., 1970, *J. chem. Soc. chem. Commun.*, 1453.
YAGI, T., INOKUCHI, H., and KIMURA, K., 1983, *Acc. chem. Res.*, **16,** 1.
ZINKE, A., and PONGRATZ, A., 1936, *Ber. deutsch. chem. Gesell.*, **69,** 1591; 1937, *Ibid.*, **70,** 214.